

# Inelastic Fracture Parameter, CED, for an Interface Crack —2nd Report, A Study Based on Elastic-plastic Finite Element Analyses—

## 界面き裂の非弾性破壊パラメータ CED

—第2報, 弾塑性有限要素解析に基づく検討—

Yutaka SATO\*, Daisuke NAGASAWA\*\* and Katsuhiko WATANABE\*

佐藤 裕・長沢 大介・渡辺 勝彦

### 1. Introduction

The objective of this research is to explore the possibility of the CED as an inelastic fracture parameter of an interface crack. In the 1st Report<sup>1)</sup>, the fundamental relations about the CED of an interface crack were introduced and, through the elastic finite element analyses of an example, it was pointed out that the Mode I and Mode II contributions of CED seem not, at least in linear elastic case, to satisfy the requirement for being crack parameters although the total CED may play the role of crack parameter.

In this report, what kinds of properties the total CED and its each Mode contribution show in elastic-plastic state, where the scale of plastic region is not so large, is studied through the finite element analyses of a specimen with a center-crack in the interface, and it is shown that, different from elastic case, the possibility of the each Mode contribution as an interface crack parameter comes out besides the total CED once yielding begins.

### 2. Finite Element Analyses

#### 2.1 Object and Method of Analyses

Bimaterial specimens with a center-crack in the interface under uniform forced displacement  $u$  shown in Fig. 1 were analysed by elastic-plastic finite element method under plane strain condition. A semicircular notch with root radius  $\rho$  is adopted as a crack model as is shown in Fig. 2 and four kinds of  $\rho/a$  are taken ( $\rho/a = 0.001, 0.004, 0.016, 0.064$ ). The combinations of material constants employed are shown in Table 1. Here,  $\mu, E$  and  $\sigma_y$  are shear modulus, Young's modulus and yielding stress respectively, and sub-scripts 1 and 2 mean the

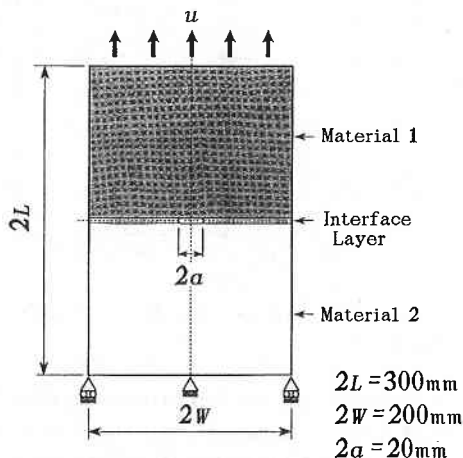


Fig. 1 Specimen Configuration

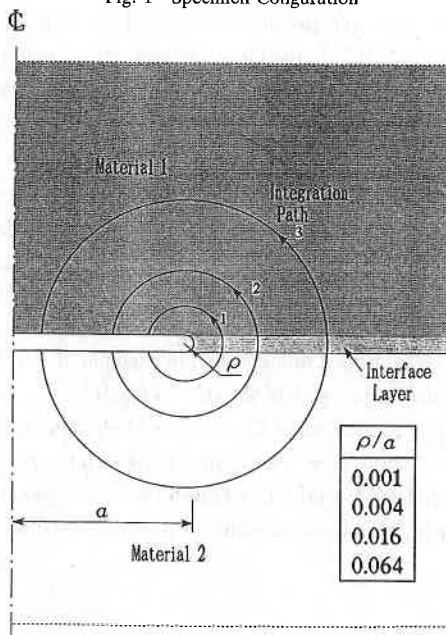


Fig. 2 Notch Model of an Interface Crack and Integration Path

\*Institute of Industrial Science, University of Tokyo

\*\*Central Japan Railway Co.

quantities of Material 1 and Material 2 respectively. Poisson's ratio is 0.3 in both materials ( $\nu_1 = \nu_2 = 0.3$ ) and strain hardening rate is taken at  $H = E / 100$  in each material. In the interface layer, its material constants are supposed to change continuously from those of Material 2 to those of Material 1<sup>1)</sup>, and the geometrical mean values are taken as the simplest approximation, that is,  $\mu_3 = \sqrt{\mu_1\mu_2}$  ( $E_3 = \sqrt{E_1E_2}$ ),  $\nu_3 = \sqrt{\nu_1\nu_2}$ ,  $\sigma_{y3} = \sqrt{\sigma_{y1}\sigma_{y2}}$ , and  $H_3 = \sqrt{H_1H_2}$ .

2.2 CED Evaluation

The CED,  $\mathcal{E}(\rho)$ , and its Mode I and Mode II contributions,  $\mathcal{E}^I(\rho)$  and  $\mathcal{E}^{II}(\rho)$ , were evaluated by  $\mathcal{E}_J$ -integral and,  $\mathcal{E}^I$ - and  $\mathcal{E}^{II}$ -integrals<sup>1)</sup>, respectively. Integration paths used in the evaluations of these domain integrals are shown in Fig. 2. It was confirmed that the path-independencies of the integrals were kept well, so the averaged values for three integration paths were taken as the values of  $\mathcal{E}_J$ ,  $\mathcal{E}^I$  and  $\mathcal{E}^{II}$ .

3. Result and Discussion

3.1 Before the Onset of Yielding

The analyses here are elastic-plastic ones, so the variations of the ratios of  $\mathcal{E}^I$  and  $\mathcal{E}^{II}$  to  $\mathcal{E}_J$  with the increase of  $\rho/a$  in elastic state before yielding are shown in Fig. 3 with the result of elastic analysis when  $\mu_1/\mu_2 = 2.0$  (elastic-plastic analysis was not carried out). In elastic case,  $\mathcal{E}_J$ -integral coincides with  $J$ -integral theoretically<sup>1)</sup> and also the agreement between them in the analyses was quite good. The dependency of  $\mathcal{E}_J$  on  $\rho$  is, as was

Table 1 Combination of Material Constants

	$\mu_1 / \mu_2=1.0$	$\mu_1 / \mu_2=5.0$	$\mu_1 / \mu_2=10.0$
$\mu_1 (E_1)$	769.2 (2000)	3846 (10000)	7692 (20000)
$\mu_2 (E_2)$	769.2 (2000)	769.2 (2000)	769.2 (2000)
$\sigma_{y1}$	15.0	35.0	70.0
$\sigma_{y2}$	15.0	15.0	15.0

Unit: [kgf/mm<sup>2</sup>]

expected<sup>1)</sup>, almost negligible, therefore, Fig. 3 shows that  $\mathcal{E}^I$  and  $\mathcal{E}^{II}$  depend on  $\rho$  ( $\mathcal{E}_J = \mathcal{E}^I + \mathcal{E}^{II}$  in definition and this was almost satisfied numerically) and this tendency becomes remarkable with the increase of  $\mu_1/\mu_2$ . The conclusion obtained from the results here is almost the same as that obtained from the results of analyses of an interface crack in an infinite plate over wider range of  $\rho/a$  in the 1st Report<sup>1)</sup>. That is,  $\mathcal{E}_J$  can be one of crack parameters because of its  $\rho$ -independency, whereas  $\mathcal{E}^I$  and  $\mathcal{E}^{II}$  can not be crack parameters until an appropriate value of  $\rho$  which should be determined depending on the combination of materials and specimen configuration is given.

3.2 After the Onset of Yielding

Figures 4, 5 and 6 show the variations of  $\mathcal{E}_J$  with the increase of loading point displacement  $u$  when  $\mu_1/\mu_2 = 1.0, 5.0$  and  $10.0$  respectively. Also after the onset of yielding, the dependency of  $\mathcal{E}_J$  on  $\rho$  is kept small in every case, and  $\mathcal{E}_J$  agrees well numerically with  $J$ -integral although there is no theoretical guarantee in a strict sense

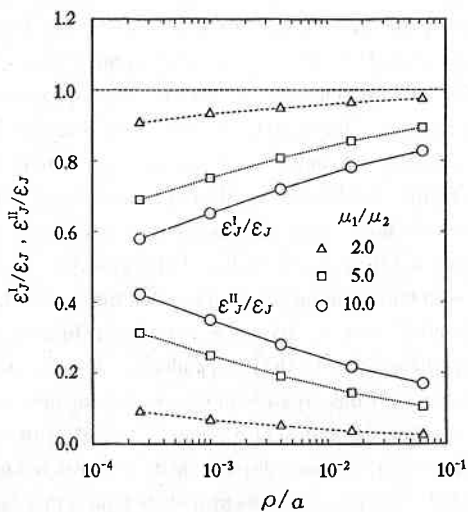


Fig. 3  $\rho$ -dependencies of  $\mathcal{E}^I$  and  $\mathcal{E}^{II}$

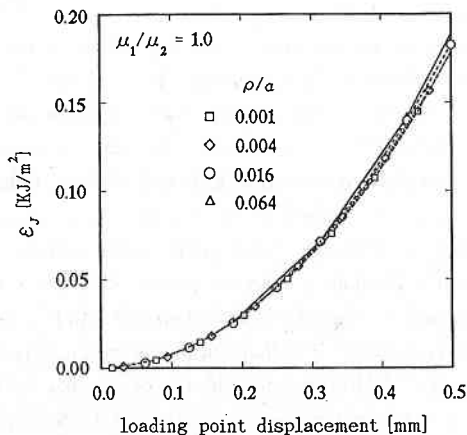


Fig. 4 Variation of  $\mathcal{E}_J$  with Loading Point Displacement ( $\mu_1/\mu_2=1.0$ )

研究速報

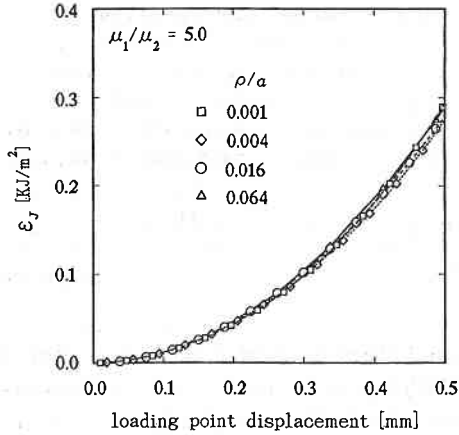


Fig. 5 Variation of  $\epsilon_J$  with Loading Point Displacement ( $\mu_1/\mu_2=5.0$ )

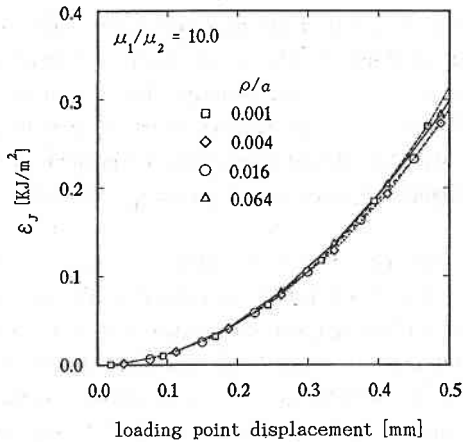


Fig. 6 Variation of  $\epsilon_J$  with Loading Point Displacement ( $\mu_1/\mu_2=10.0$ )

in elastic-plastic case (the values of  $J$  are not shown to avoid the intricacies in the figures). The results here mean that  $\epsilon_J$  can be a crack parameter also in elastic-plastic state as it could be in elastic state. In order to grasp the degree of plastic deformation dealt with here, an example of plastic zone is shown in Fig. 7, where  $\sigma_m$  is averaged nominal stress when  $u = 0.469$  mm. As the analyses are up to  $u = 0.5$  mm, it is known that the case where the plastic zone size is not so large compared with the crack length is discussed. The shape of plastic zone is different for each  $\rho/a$ . However, the differences are small except immediately after the onset of yielding and the outlines of plastic zone become almost the same rapidly with the progress of plastic deformation.

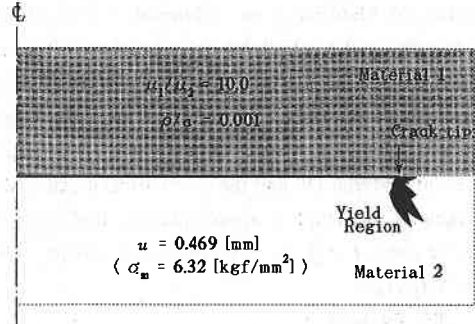


Fig. 7 An Example of Plastic Region around an Interface Crack Tip

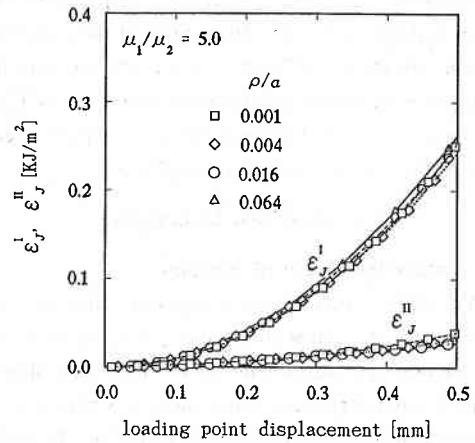


Fig. 8 Variations of  $\epsilon_J^I$  and  $\epsilon_J^{II}$  with Loading Point Displacement ( $\mu_1/\mu_2=5.0$ )

It has been concluded that  $\epsilon_J$  can play the same role also after the onset of yielding as in elastic state. Then, how are  $\epsilon_J^I$  and  $\epsilon_J^{II}$ ? Figures 8 and 9 show how  $\epsilon_J^I$  and  $\epsilon_J^{II}$  increase with the increase of loading point displacement when  $\mu_1/\mu_2 = 5.0$  and  $10.0$  respectively. It goes without saying that  $\epsilon_J^I = \epsilon_J$  and  $\epsilon_J^{II} = 0$  when  $\mu_1/\mu_2 = 1.0$ . From these figures, it is known that the dependencies of  $\epsilon_J^I$  and  $\epsilon_J^{II}$  on  $\rho$  are not so large different from in elastic case and it seems that they can be neglected in engineering sense. This is an important fact and implies that the possibilities of  $\epsilon_J^I$  and  $\epsilon_J^{II}$  as crack parameters come out. In order to explain the reason why the  $\rho$ -dependencies in elastic state disappear with the progress of plastic deformation, the variations of the ratios of  $\epsilon_J^I$  and  $\epsilon_J^{II}$  to  $\epsilon_J$  with the increase of loading point displacement are shown in Figs. 10 and 11. That is, it is known from these figures that each of  $\epsilon_J^I/\epsilon_J$  and  $\epsilon_J^{II}/\epsilon_J$  tends to approach some constant

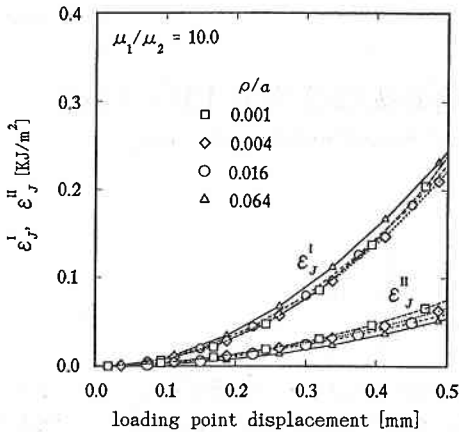


Fig. 9 Variations of  $\mathcal{E}^I_J$  and  $\mathcal{E}^{II}_J$  with Loading Point Displacement ( $\mu_1/\mu_2=10.0$ )

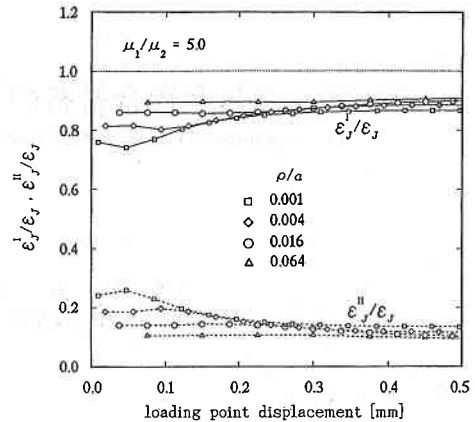


Fig. 10 Variations of  $\mathcal{E}^I_J/\mathcal{E}_J$  and  $\mathcal{E}^{II}_J/\mathcal{E}_J$  with Loading Point Displacement ( $\mu_1/\mu_2=5.0$ )

value independent of  $\rho$  with the progress of plastic deformation and, as  $\mathcal{E}_J$  depends little on  $\rho$ , the  $\rho$ -dependencies of  $\mathcal{E}^I_J$  and  $\mathcal{E}^{II}_J$  disappear in Figs. 8 and 9.

Although it is necessary to study various types of problem further to reach a final conclusion, the possibilities of Mode I and Mode II contributions of CED as well as the total CED as crack parameters have come out in elastic-plastic state. Considering that the fracture problem of a mixed-mode crack in a homogeneous material could be explained successfully by Mode I and Mode II contributions of CED<sup>2)</sup>, it may be possible to explain also the elastic-plastic fracture of an interface crack by Mode I and Mode II contributions of CED.

#### 4. Conclusion

The properties of the total CED and its Mode I and Mode II contributions of an interface crack were studied through the elastic-plastic finite element analyses of an example problem. It has been shown that not only  $\mathcal{E}_J$  but also  $\mathcal{E}^I_J$  and  $\mathcal{E}^{II}_J$  may be expected to be crack parameters in elastic-plastic state. (Manuscript received, June 25, 1993)

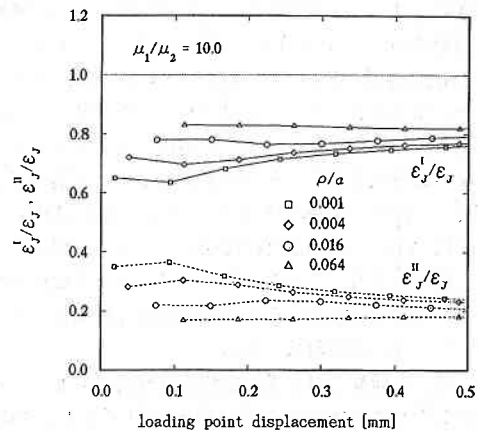


Fig. 11 Variations of  $\mathcal{E}^I_J/\mathcal{E}_J$  and  $\mathcal{E}^{II}_J/\mathcal{E}_J$  with Loading Point Displacement ( $\mu_1/\mu_2=10.0$ )

#### References

- 1) Watanabe, K., Sato, Y. and Nagasawa, D., Seisan-Kenkyuu (to be published).
- 2) Watanabe, K. and Utsunomiya, T., Int. J. of Pressure Vessel and Piping, 44 (1990), p. 175.